Electronic Supplementary Material (ESI) for Journal of Materials Chemistry A.

Supporting Information

Three-dimensional Printed Cellular Stainless Steel as High-activity Catalytic Electrode for Oxygen Evolution

Xiaolei Huang+, Shuai Chang+, Wee Siang Vincent Lee, Jun Ding*, and Jun Min Xue*

Department of Materials Science and Engineering, Faculty of Engineering, National University of Singapore, 9 Engineering Drive 1, Singapore 117576, Singapore.

E-mail: msedingj@nus.edu.sg (Jun Ding); msexuejm@nus.edu.sg (Jun Min Xue)

[+] These authors contributed equally to this work.

Experimental Section

Fabrication of cellular stainless steel and planar stainless steel: Electrode design was firstly drawn using Solidworks 2015 3D modeling software. Metal 3D printing was carried out with a SLM®280HL (SLM Solutions GmbH, Germany) which uses a SLM technique. A focused, high-energy fiber laser beam with a wavelength of 1070 nm fuses and links metallic particles deposited in powder form on a printing stage according to the established design in a layer by layer fashion. The chamber is filled with nitrogen to avoid material oxidation. Spherical stainless steel powder (SLM Solutions GmbH, Germany) were employed to produce stainless steel electrodes. Electrochemical polishing of CESS and PSS samples were performed, the electrolyte is the phosphoric-sulfuric mixed acid with volume ratio of 2:1. Potentiostatic polishing of samples was performed at 1.8 V (vs. Ag/AgCl) for 30 minutes at temperature of 50 °C. The electrolyte solution is circulating in the bath driven by magnetic stirring, so that the surface especially the inner face can be processed uniformly. For comparison, commercial stainless steel foam (CSSF) were obtained from Baoji Intelle Metals Co., Ltd.

Characterization: SEM was performed on ZEISS SEM Supra 40. XPS analysis was carried on an Axis Ultra DLD X-ray photoelectron spectrophotometer. The mechanical properties of samples were evaluated by EZ50, LLOYD INSTRUMENTS. The electronic conductivity of samples was measured by a four-probe method. Porosity was accomplished by weighing combined with Archimedes' method. A micro-CT scanner (Quantum Fx μCT, Caliper Life Sciences) at 20 μm resolution using 90 kV voltage and

180 μA current was used to scan the cellular structures, and 2D slice image data were collected. AMIDE software was used to reconstruct the 3D models of the fabricated lattice structures using the 2D slice images data obtained from micro-CT scans.

Electrochemical measurements: The electrochemical experiments were performed using a VMP3 electrochemical workstation (Bio-logic Inc). All electrochemical measurements were conducted in a typical three-electrode setup using catalytic electrode as the working electrode, a graphite plate as the counter electrode and an Hg/HgO electrode (1M KOH) as the reference electrode. LSV measurements were conducted in 1M KOH with a scan rate of 5 mV s^{-1} at room temperature to minimize the capacitive current. Before recording, the potential of catalytic electrode was scanned for 20 cycles until a stable LSV was recorded. Chronopotentiometry was carried out under a current density of 40 mA cm^{-2}. Every 1 h recorded an impedance measurement, after 11h, every 5 h recorded an impedance measurement for chronopotentiometry. Electrochemical impedance spectroscopy (EIS) measurements of the samples were carried out above three electrode systems. The frequency range was 100 mHz to 700 kHz, and the amplitude of the applied voltage was 5 mV. The potentials recorded for LSV and chronopotentiometry have been calibrated with respect to a reversible hydrogen electrode (RHE). The electrochemical double-layer capacitance (EDLC) of electrode was measured by CV scans at various scan rated within the potential window where there is a non-Faradic current response. The current density at 0 V vs. Hg/HgO was plotted against scan rate and the slope of the linear fit curve is the EDLC (C_{DL}). The electrochemically active surface area (*ECSA*) was calculated from C_{DL} according to:

$$ECSA\ (cm^2) = \frac{C_{DL}}{C_s}$$

Where C_s is the capacitance of an atomically smooth planar surface of the material per unit area under identical electrolyte conditions. A value of $C_s = 0.04$ mF cm^{-2} was used based on previously reported value.[1]

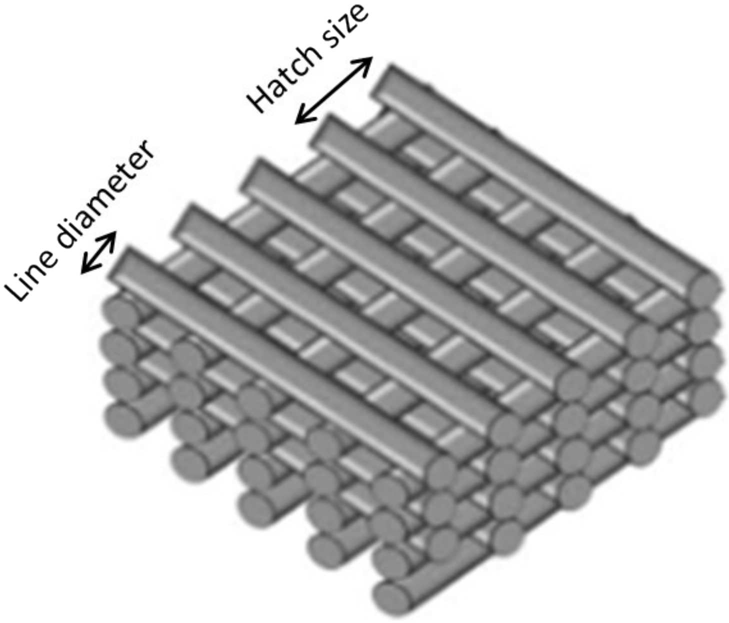

Figure S1. The mesh model used for selective laser melting.

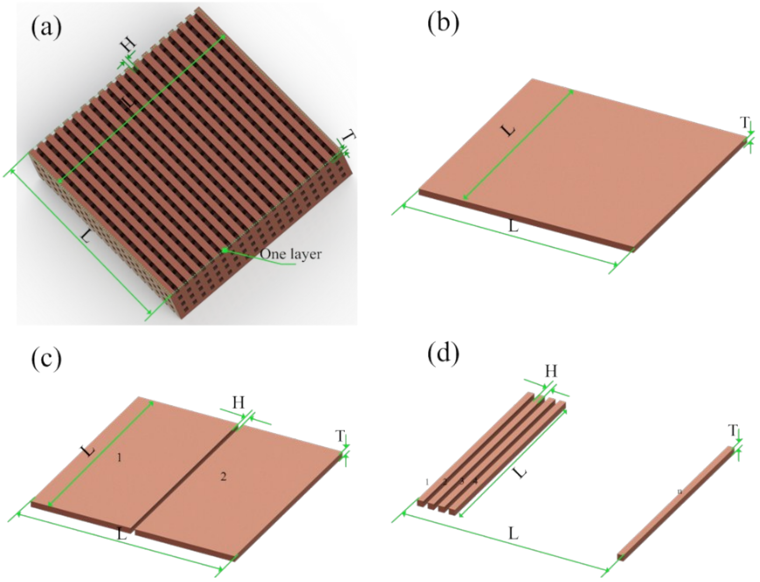

Figure S2. (a) Scheme of the cellular structure with 3D dimensioning. (b) One layer of dense plate. (c) One layer of two separated plates. (d) One layer constituted by N bars. In this work, the length (L) and width (L) of the cellular sample are all 10mm, the thickness (T) of one layer is 0.25mm, and the separation distance (H) of the neighbouring bars is 0.2mm. The numbers of the bars in one layer is n.

The surface area of one layer of dense plate:

$S(1) = 2L^2 + 4LT$

The surface area of one layer of two separated paltes:

$S(2) = 2L^2 + 4LT + 2(LT - HL - HT)$

where $LT - HL - HT = 10 \times 0.25 - 10 \times 0.2 - 0.2 \times 0.25 = 0.45 > 0$

then $S(2) > S(1)$.

The surface area of one layer constituted by N bars:

$S(n) = 2L^2 + 4LT + 2(n-1)(LT - HL - HT)$

where $LT - HL - HT > 0$

then the surface area (S) is positive correlation with the numbers (n) of bars.

The diameter (width) of one bar:

$W = (L + H) / n + H$

So the surface area (S) is also negative correlation with diameter (width) of one bar.

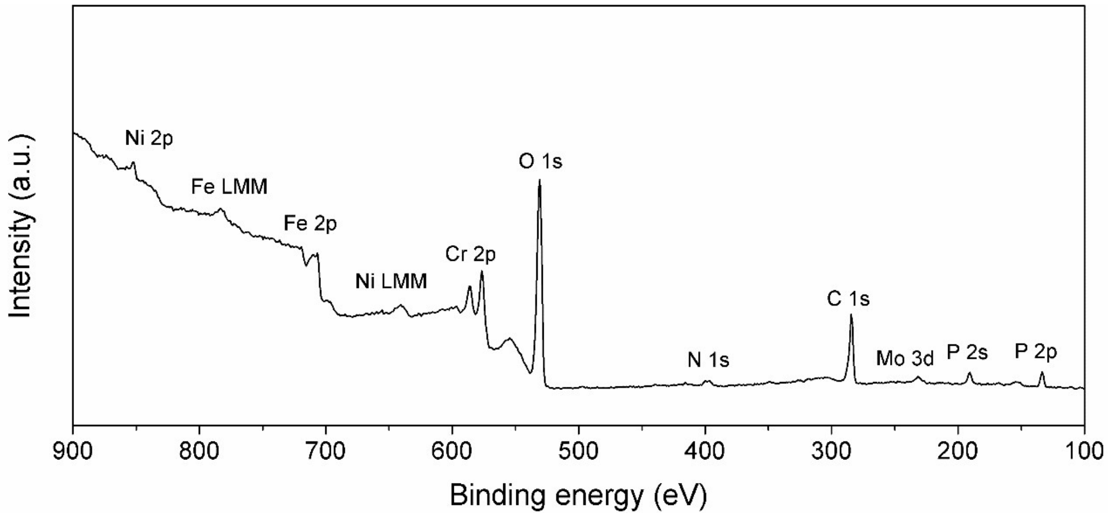

Figure S3. Wide-scan XPS spectrum of CESS.

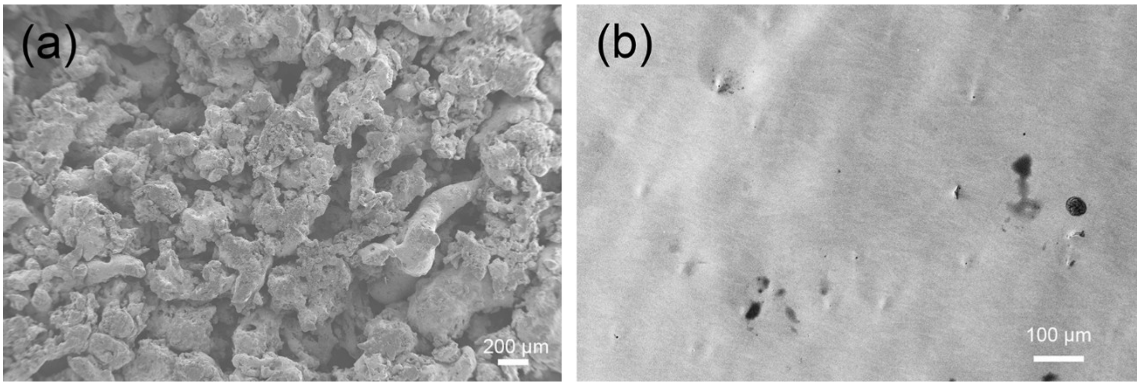

Figure S4. The SEM image of (a) CSSF and (b) PSS.

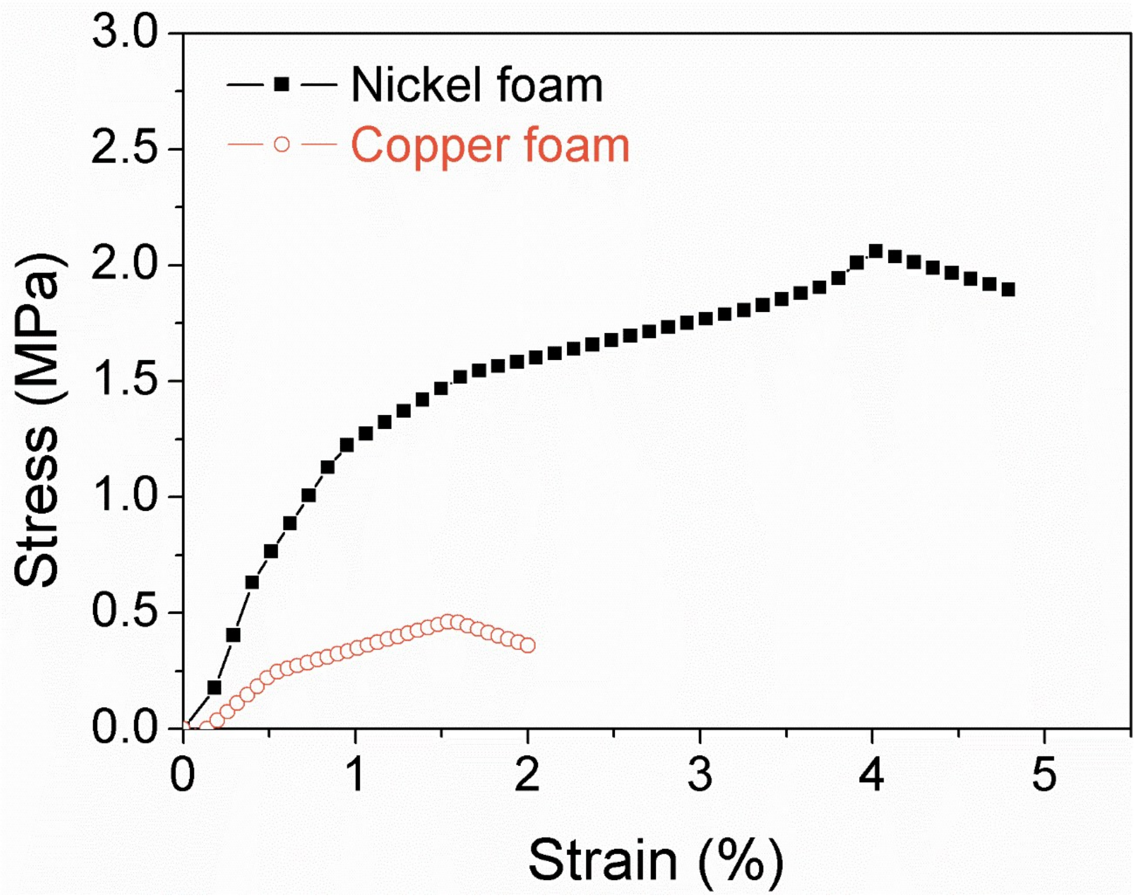

Figure S5. The tensile stress-strain curves of commercial nickel foam and copper foam.

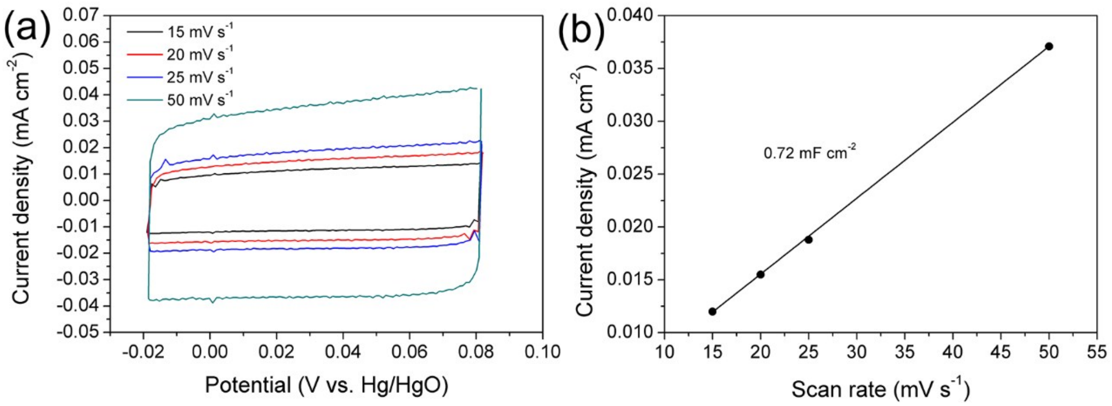

Figure S6. (a) Cyclic voltammograms of nickel foam at different scan rate from 15 to 50 mV s^{-1}. (b) Cathodal current measured at 0 V (vs. Hg/HgO) as a function of scan rate for nickel foam.

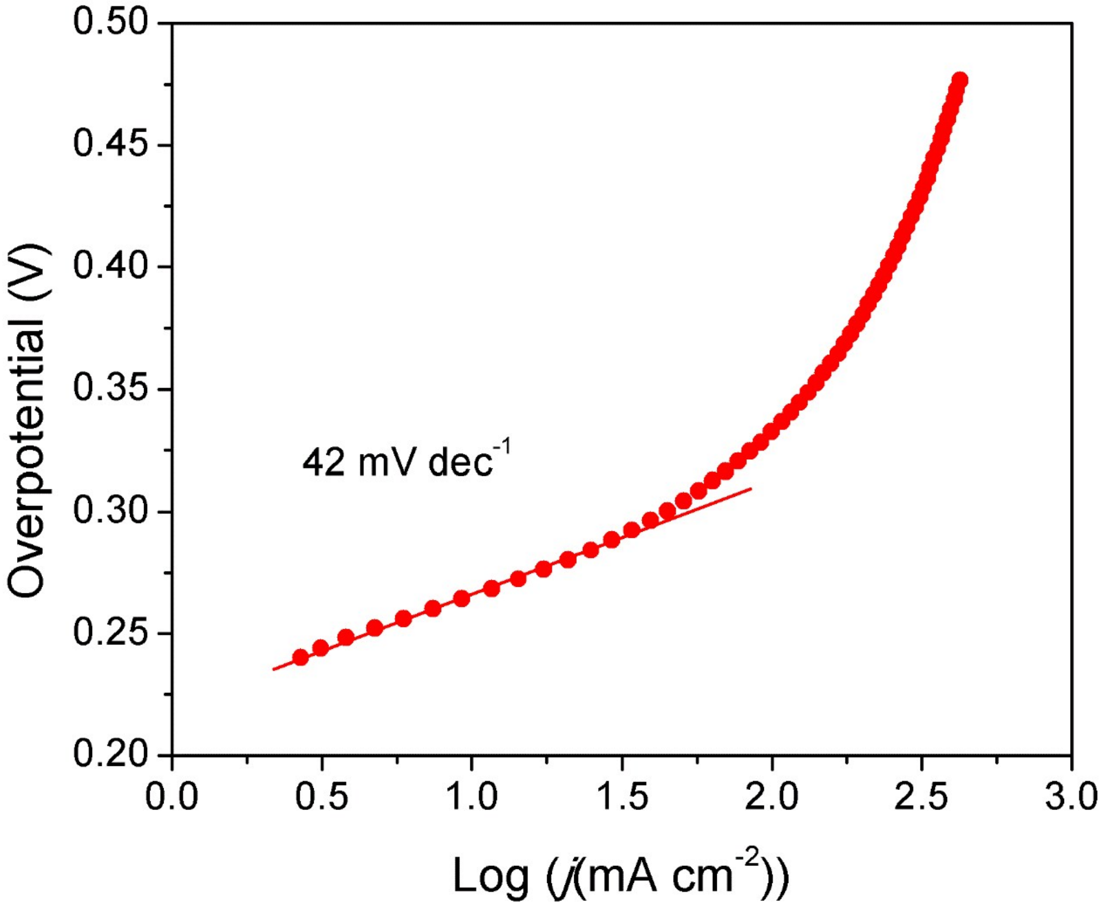

Figure S7. Tafel plots for CESS after 10,000th LSV cycles.

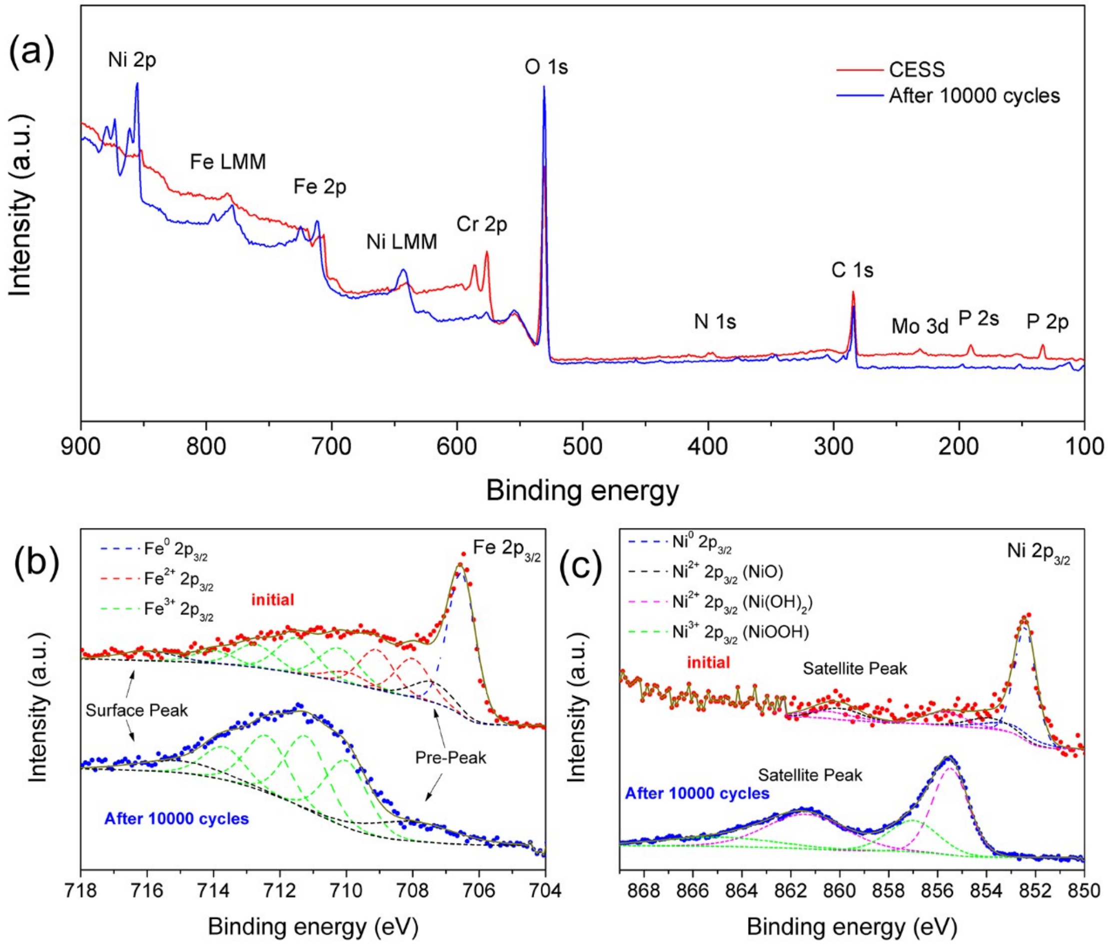

Figure S8. (a) Wide-scan XPS spectrum of CESS before and after 10,000th LSV cycles. (b) Fe 2p, and (c) Ni 2p XPS spectra of CESS before and after 10,000th LSV cycles.

Table S1: Summary of the OER activities of 3D electrode.

Sample	**Overpotential at 10 mA cm^{-2} (mV)**	**Tafel Slopes ($mV\ dec^{-1}$)**	**Reference**
3D printed cellular stainless steel electrode	302 (before activation)[a]	43[a]	This work
3D printed cellular stainless steel electrode	270 (after activation)[a]	42[a]	This work
3D porous carbon microtube sponge	290	246	[2]
Oxidized carbon cloth	477	82	[3]
3D N-doped porous carbon cloth	360	98	[4]
N, S codoped graphite foam	346	78	[5]
G-FeCoW on gold foam	191[a]	223[a]	[6]
Ni-phytate on Ni foam	280	40	[7]
$NiCo_2S_4$ on Ni foam	260	40.1	[8]
NiFe LDH on Ni foam	240	–	[9]

[a] Obtained from polarization curves (based on geometric area) without *iR* correction.

Reference:

[1] a) Y. Yang, H. Fei, G. Ruan, J. M. Tour, *Adv. Mater.*, 2015, **27**, 3175; b) X. Lu, W. Yim, B. H. R. Suryanto, C. Zhao, *J. Am. Chem. Soc.*, 2015, **137**, 2901.

[2] J. Li, P. Hou, S. Zhao, C. Liu, D. Tang, M. Cheng, F. Zhang, H. Cheng, *Energy Environ. Sci.*, 2016, **9**, 3079.

[3] N. Cheng, Q. Liu, J. Tian, Y. Xue, A. M. Asiri, H. Jiang, Y. He, X. Sun, *Chem. Commun.*, 2015, **51**, 1616.

[4] M. Balogun, W. Qiu, H. Yang, W. Fan, Y. Huang, P. Fang, G. Li, H. Ji, Y. Tong, *Energy Environ. Sci.*, 2016, **9**, 3411.

[5] X. Yu, M. Zhang, J. Chen, Y. Li, G. Shi, *Adv. Energy Mater.*, 2015, 1501492.

[6] B. Zhang, X. Zheng, O. Voznyy, R. Comin, M. Bajdich, M. García-Melchor, L. Han, J. Xu, M. Liu, L. Zheng, F. P. G. d. Arquer, C. T. Dinh, F. Fan, M. Yuan, E. Yassitepe, N. Chen, T. Regier, P. Liu, Y. Li, P. D. Luna, A. Janmohamed, H. L. Xin, H. Yang, A. Vojvodic, E. H. Sargent, *Science*, 2016, **352**, 333.

[7] X. Chen, G. Zeng, T. Gao, Z. Jin, Y. Zhang, H. Yuan, D. Xiao, *Electrochem. Commun.*, 2017, **74**, 42.

[8] A. Sivanantham. P. Ganesan, S. Shanmugam, *Adv. Funct. Mater.*, 2016, **26**, 4661.

[9] J. Luo, J. Im, M. T. Mayer, M. Schreier, M. K. Nazeeruddin, N. Park, S. D. Tilley, H. J. Fan, M. Grätzel, *Science*, 2014, **345**, 1593.